Arabian Journal for Science and Engineering (2023) 48:7587–7601
https://doi.org/10.1007/s13369-022-07588-6

RESEARCH ARTICLE-CHEMISTRY

Novel Cytocompatible Chitosan Schiff Base Derivative as a Potent Antibacterial, Antidiabetic, and Anticancer Agent

Ahmed M. Omer[1] · Abdelazeem S. Eltaweil[2] · Esmail M. El-Fakharany[3] · Eman M. Abd El-Monaem[2] · Magda M. F. Ismail[4] · Mohamed S. Mohy-Eldin[1] · Mohammed S. Ayoup[2]

Received: 29 August 2022 / Accepted: 20 December 2022 / Published online: 12 January 2023

Abstract

This study intends to develop a novel bioactive chitosan Schiff base (CTS-SB) derivative via coupling of chitosan (CTS) with 4-((5, 5-dimethyl-3-oxocyclohex-1-en-1-yl) amino) benzene-sulfonamide. The alteration in the chemical structure of CTS-SB was verified using ^{1}H NMR and FT-IR analysis, while the thermal and morphological properties were inspected by TGA and SEM characterization tools, respectively. Ion exchange capacity of the developed CTS-SB derivative recorded a maximal value of 12.1 meq/g compared to 10.1 meq/g for pristine CTS. In addition, antibacterial activity of CTS-SB derivative was greatly boosted against *Escherichia coli* (*E coli*) and *Staphylococcus aureus* (*S. aureus*) bacteria. Minimum inhibition concentration of CTS-SB derivative was perceived at 50 μg/mL, while the highest concentration (250 μg/mL) could inhibit the growth of *S. aureus* up to 91%. What's more, enhanced antidiabetic activity by CTS-SB derivative, which displayed higher inhibitory values of α-amylase (57.9%) and α-glucosidase (63.9%), compared to those of pure CTS (49.8 and 53.4%), respectively Furthermore, cytotoxicity investigation on HepG-2 cell line revealed potential anticancer activity along with good safety margin against primary human skin fibroblasts (HSF cells) and decent cytocompatibility. Collectively, the gained results hypothesized that CTS-SB derivative could be effectively applied as a promising antibacterial, anticancer and antidiabetic agent for advanced biomedical applications.

Keywords Chitosan · Schiff base · Antibacterial · Anticancer · Antidiabetic · Cytotoxicity

1 Introduction

More recently, much attention being oriented to the use of biopolymers- in various biomedical applications [1], owing to their appealing characteristics comprising low-cost production, availability in nature, biodegradability, biocompatibility and non-toxicity [2, 3]. Among them, chitosan (CTS) is a naturally occurring marine biopolymer that is acquired by N-deacetylation of chitin which is the principal structural polymer in arthropod exoskeletons [4]. Chitosan has three types of reactive groups present in its distributed (1-4)-linked 2-amino-2-deoxy-β -d-glucopyranose structure units, namely, the primary amine groups, the primary and secondary hydroxyl groups at C-2, C-3, and C-6 positions, respectively [5]. The primary NH_2 group of the glucosamine residues is the most substantial reactive functional group for the biological asset of chitosan [6]. Therefore, chitosan has been considered the key to the massive majority of various biomedical and industrial applications including wound

✉ Ahmed M. Omer
amomar@srtacity.sci.eg

✉ Abdelazeem S. Eltaweil
abdelazeemeltaweil@alexu.edu.eg

✉ Mohammed S. Ayoup
Mohamed.salah@alexu.edu.eg

1 Polymer Materials Research Department, Advanced Technologies and New Materials Research Institute (ATNMRI), City of Scientific Research and Technological Applications (SRTA-City), P.O. Box 21934, New Borg El-Arab City, Alexandria, Egypt

2 Department of Chemistry, Faculty of Science, Alexandria University, P.O. Box 426, Ibrahimia 21525, Alexandria, Egypt

3 Protein Research Department, Genetic Engineering and Biotechnology Research Institute, City of Scientific Research and Technological Applications (SRTA-City), P.O. Box 21934, New Borg El-Arab City, Alexandria, Egypt

4 Department of Pharmaceutical Medicinal Chemistry, Faculty of Pharmacy (Girls), Al-Azhar University, Cairo 11651, Egypt

dressing, drug delivery, tissue engineering and water treatment [7–10].

Moreover, chitosan has encouraging ambitious biological activities such as antimicrobial, antitumor, anticoagulants, antioxidant, anti-inflammatory and hemostatic impacts [11–13]. Chitosan plays also a crucial role in the cytotoxic profile and targeting of cancers that are characterized by rapid division and aggressive growth [14]. Additionally, chitosan displays respectable antimicrobial activity against various types of microorganisms, since it has the aptitude to form a strong barrier-based film for hindering their attacking [15]. Nevertheless, the antimicrobial activity of chitosan has become gradually suppressed as a result of the non-stop mutations of microorganisms to resist the activity of antibiotics [16, 17]. Numerous physicochemical modification techniques including quaternization, grafting, functionalization with bioactive compounds and Schiff base formation have been conducted to improve the biological activities of chitosan for widen its range of applications [18–20]. The last efficacious technique involves the superficial reaction of active carbonyl compounds such as aldehydes and ketones with the free active amine groups of chitosan to form Schiff bases with an imine moiety (–RC = N–) [21]. Chitosan Schiff base derivatives have continuously getting over the top consideration due to the assessment of their organic solicitations, which exhibited more potent antimicrobial and antioxidant activities compared to neat chitosan [22]. For instance, the developed Schiff bases from the reaction of chitosan with aldehydes such as benzaldehyde [23], crotanaldehyde [21] and salicylaldehyde [24] exposed greater activities against various types of bacteria. The authors' previous studies also proved the adequate antimicrobial, antioxidant and anti-inflammatory activities of the Schiff bases resultant from the reaction of chitosan with 4- chlorobenzaldebyde, isatin and Indole-3-carboxaldehyde [20, 22, 25].

Besides, potentials of Schiff bases-based chitosan have been established with special reference to their capabilities for improvement the inhibition rate of the growth of the cancer cell [26]. Further, chitosan and its derivatives have encouraged antidiabetic activities, which are mediated over various mechanisms comprising suppression of α-glucosidase and α-amylase activities, glucose metabolism and reduced β-cell dysfunction [27]. Therefore, Schiff bases demonstrated also tolerable antidiabetic activity in the presence of aromatic substituent and phenolic functional groups [28].

On the other hand, sulfonamide-containing drugs have broad applications in biomedical fields [29, 30] as potent compounds for blocking tumor growth and inhibit angiogenesis. Besides, sulfonamide-based Schiff bases compounds demonstrate significant antimicrobial activities against pathogenic bacteria such as *Staphylococcus aureus, Streptococcus pyogenes, Methicillin-resistant Staphylococcus aureus, Escherichia coli* and *Klebsiella pneumoniae*, in addition to pathogenic fungi including *Candida tropicalis* and *Trichophyton rubrum* [31, 32].

The aim of this study is to synthesize a new chitosan-sulfonamide conjugate via dimidone linker, since carbonyl of dimidone (enolic form) can condensed with primary NH_2 functionality of CTS to yield Schiff's base, while the enolic OH is condensed with the basic NH_2 group of sulfonamide**.** The chemical structure, thermal properties and morphological changes of the developed Schiff base were inspected. In addition, we herein attempted to synergize the antibacterial, antidiabetic and anticancer activities of pure CTS with that of sulfonamide moiety. Moreover, cytotoxicity on Human Skin Fibroblast Cells (HSF) and hemodialysis investigation were performed to ensure compatibility and safety of the as-fabricated CTS Schiff base derivative.

2 Experimental

2.1 Materials

Chitosan (DD = 95%, M.wt. 100000–300000D), dimidone (5,5-Dimethyl-1,3-cyclohexanedione; assay 95%), sulfanilamide (assay ≥ 98%), MTT (3-(4, 5-dimethyl-2-thiazolyl)-2,5-diphenyl-2H- tetrazolium bromide, 98%), peptone (≥ 10% nitrogen), yeast extract (for microbial growth medium), bovine serum albumin (BSA, assay ≥ 98%), glucose (~ 20% in H_2O), α –amylase (1.5 U/mg), ρ-nitrophenyl-α-D-glucoside (assay ≥ 99%), potassium iodide (assay ≥ 99.0%), dimethyl sulfoxide (DMSO, assay ≥ 99.9%), berberine chloride (primary reference standard), citrate-dextrose solution (ACD.) were provided by Sigma Aldrich Co. (Germany). Glacial acetic acid (assay 95%), sulfuric acid (assay 98%), hydrochloric acid (purity 37%), sodium chloride (assay 98%), sodium carbonate (assay 85%), sulfuric acid (purity 98%), sodium hydroxide (assay 98%) and ethyl alcohol (purity 98%) were delivered by El-Nasr Co. (Egypt).

2.2 Synthesis of Chitosan Schiff Base (CTS-SB)

4-((5, 5-dimethyl-3-oxocyclohex-1-en-1-yl) amino) benzene-sulfonamide was firstly synthetized by reflux of dimedone (1 mmol) and Sulfanilamide (1 mmol) in ethanol (50 mL). The reaction was conducted for 4 h, then left to cool at room temperature. The resultant precipitate was filtered and air-dried as colorless crystals. The Schiff base derivative was synthetized according to the authors' previously reported method with a slight modification [25, 33]. In brief, an accurate quantity of CTS was dissolved at room temperature in 50 mL of glacial acetic acid (2%; w/v) under gentle stirring. Thereafter, the prepared 4-((5,

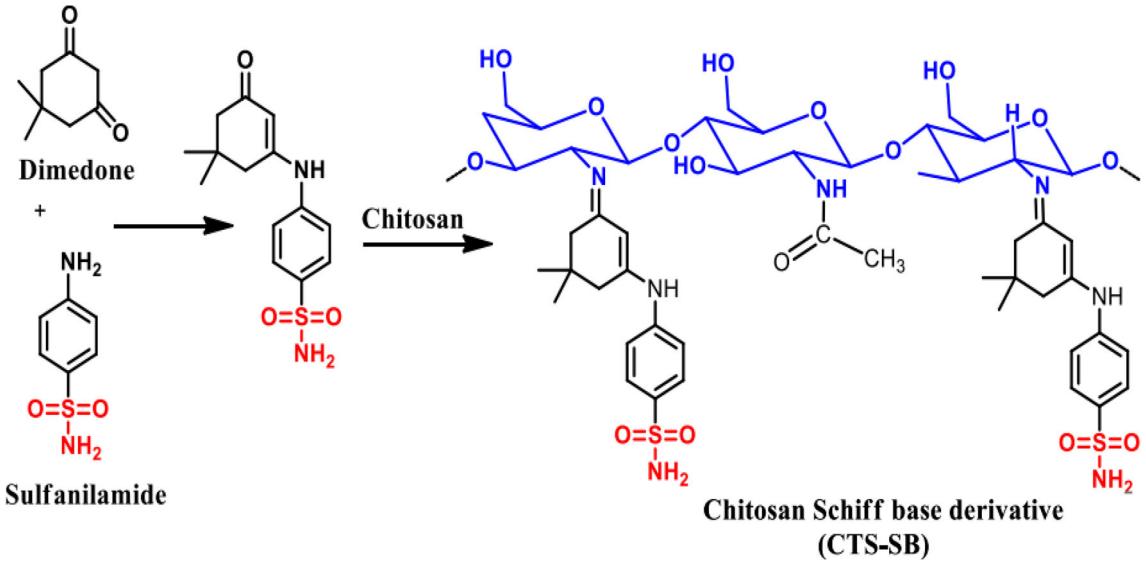

Fig. 1 Mechanistic pathway for the synthesis of CTS-SB derivative

5-dimethyl-3-oxocyclohex-1-en-1-yl) amino) benzene-sulfonamide was dissolved in 10 mL of ethyl alcohol and subsequently added into CTS solution. The reaction mixture was stirred for 8 h at 80 °C, since a pale-yellow color was generated as a result of Schiff base formation. The resultant product was precipitated in the powder form by neutralization using Na_2CO_3 and ethyl alcohol (50 mL). Finally, the synthesized chitosan Schiff base powder was collected by centrifugation, washed several times using distilled water and ethyl alcohol to eliminate the un-reacted substances and finally by vacuum-drying at 60 °C overnight. The developed Schiff base was coded as CTS-SB, while the reaction mechanism is depicted in Fig. 1.

2.3 Instrumental Characterization

The changes in the chemical structures of CTS and the newly Schiff base derivative were proved by Nuclear Magnetic Resonance (1H NMR; 400 MHz, Bruker DRX-400 spectrometer), Fourier transform infrared spectroscopy (FT-IR; Model 8400 S, Shimadzu, Japan). In addition, the thermal stability of the synthetized Schiff base was examined by Thermogravimetric Analyzer (TGA; Model 50/50H, Shimadzu, Japan), while the morphological changes were inspected by a Scanning Electron Microscope (SEM; Model Jsm 6360 LA, Joel, Japan).

2.4 Ion Exchange Capacity (IEC)

Ion exchange capacity measurements were conducted according to the author's published work [20]. In brief, a known amount of tested sample was added at room temperature into 0.1 M of H_2SO_4 solution and kept for 12 h. Next, the mixture was filtered, while aliquot was titrated against 0.1 M of NaOH solution. IEC was measured depending on the following equation:

$$\mathrm{IEC(meq/g)} = \frac{(V_2 - V_1)N}{w} \tag{1}$$

where V_1 and V_2 are the needed volumes of NaOH to reach neutralization of H_2SO_4 in the absence and in the existence of the tested sample, respectively. N is the normality of NaOH solution and w is the weight of examined sample.

2.5 Antibacterial Activity Studies

To evaluate the antibacterial activity of the synthetized CTS-SB derivative, *Escherichia coli* (*E. coli*) and *Staphylococcus aureus* (*S. aureus*) were selected as gram-negative and gram-positive bacteria, respectively [34]. Bacteria were firstly refreshed via their incubation in Luria Betani (LB) culture medium (pH 7) containing of peptone (1%), yeast extract (0.5%) and NaCl (1%). The incubation was kept overnight at 37 °C under constant shaking speed (150 rpm). An exact amount of tested sample was immersed in the diluted suspension and then sterilized at 121 °C for 30 min. Consequently, the medium was kept for 24 h under shaking at 37 °C. The bacterial culture free of tested sample was used as a control. The experiment was conducted in triplicate, while the inhibition (%) was measured at 620 nm by determination the absorbance of the culture medium using a visible-spectroscopy according to the following equation [15]:

$$\text{Inhibition } (\%) = \frac{\mathrm{Abs}_a - \mathrm{Abs}_b}{\mathrm{Abs}_a} \times 100 \tag{2}$$

where Abs_a and Abs_b signify the absorbance in the absence and in the existence of tested sample, respectively.

2.6 Minimum Inhibitory Concentration Assay

The least concentration of examined sample that can entirely inhibit the bacterial growth is named minimum inhibitory concentration (MIC), which was assayed using the micro-dilution method [35]. Briefly, the bacterial strains were cultured in LB broth overnight under shaking rate of 150 rpm at 37 °C. The bacterial cultures were diluted up to 100 times by LB medium. Thereafter, an accurate quantity of examined sample (25–250 μg/mL) was soaked in sterile 96-well microplate having 20 μl of the bacterial culture suspensions. The wells were completed to 200 μl with LB broth free medium, shacked at 100 rpm for 2 min and followed by aerobic incubation overnight at 37 °C. The positive and negative controls were prepared individually by mixing the examined samples and the diluted bacterial cultures with the free LB medium, respectively. Finally, the microtiter plates were agitated for 30 s via a microplate reader before estimation of the turbidity of bacterial growth at 620 nm using a visible-spectroscopy. The experiments were performed in triplicate, and the results were represented graphically, since MIC was recorded as a function of the optical density.

2.7 Antidiabetic Studies

2.7.1 Glucose Uptake by HepG-2 Cells

Determination of glucose utilization by HepG-2 cell line was performed according to the reported method [36]. HepG-2 cells were cultured in a sterile 96-well culture micro-plate at concentration of 1×10^4 cells/well and incubated overnight in 5% CO_2 incubator at 37 °C and 90% humidity. The prepared CTS Schiff base derivative solution (5–50 μg/mL) were added to the cells and followed by incubation for 48 h at the same conditions. The culture medium was substituted with RPMI-1640 medium comprising BSA (0.1%) and glucose (8 mM) and incubated for further 3 h at 37 °C. An exact 10 μL of the medium was injected into a new 96-well plate comprising glucose oxidase reagent and incubated for 15 min at 37 °C. After incubation, the optical density (OD) was estimated at 492 nm via an ELISA microplate reader. Both negative reference (Untreated cells) and positive reference (cells treated with berberine at the same concentrations) were included. The glucose uptake (%) in HepG-2 cells was calculated according to the following equation:

$$\text{Gglucose uptake } (\%) = (\text{OD}_S - \text{OD}_C) \times 100 \tag{3}$$

where OD_S and OD_C ore the optical densities of sample and control, respectively.

2.7.2 Glucose Uptake by Yeast Cells

In order to estimate the glucose utilization in yeast cells, the clear suspension of the yeast cells was prepared by washing the yeast cells three times with deionized water until the yeast suspension became clear. Different concentrations (5, 10, 15, 20, 25 and 50 μg/mL) of the prepared CTS Schiff base derivative were added to 180 μL of the prepared glucose solution (25 mM). After incubation for 10 min at 37 °C, the reaction was started by adding 20 μL of yeast suspension. All tested mixtures were well-shaken and incubated for further 3 h at 37 °C. The tested yeast cells were precipitated by centrifugation for 5 min at 3000 rpm, while the glucose uptake was determined in the supernatant. Berberine drug was used as a standard drug, while the untreated Yeast cells were used as control cells. The percentage of glucose uptake by yeast cells was determined by a visible-spectroscopy as a function of the optical density using Eq. (3):

2.7.3 α-Amylase Inhibition Assay

The inhibition of α-amylase was assayed according to the authors previous work [37]. Briefly, α -amylase solution was prepared by dissolving the enzyme (0.5 mg/mL) in phosphate buffer (20 mM; pH 7.2). CTS Schiff base derivative (15–240 mg/mL) was added to 1 mL of the prepared enzyme solutions and the mixtures were incubated at 37 °C for 10 min. Next, the mixtures were further incubated at room temperature for 10 min after adding 1 mL of 0.5% soluble starch solution. The reaction was stopped by adding 0.5 mL of 1 M HCl, and followed by adding iodine solutions (0.1% and potassium iodide 0.01% iodine). A blank comprising phosphate buffer instead of the examined sample solution and a positive control (acarbose) at various concentrations were involved. Furthermore, no starch control and no enzyme control were included for each test sample. The OD was measured at 660 nm using a visible-spectroscopy, while the percentage inhibitory of α -amylase activity was measured according to the following equation:

$$\alpha - \text{amylase inhibition}(\%) = \left[1 - \frac{\text{OD}_s - \text{OD}_b}{\text{OD}_c}\right] \times 100 \tag{4}$$

where, OD_S, OD_b and OD_C are the optical densities of the tested sample, blank and control, respectively.

2.7.4 α-Glucosidase Inhibition Assay

An accurate 50 μL of the examined CTS Schiff base derivative (15–240 mg/mL) was added to 1 mL of α-glucosidase solution (50 μg/mL in phosphate buffer, pH 6.8). After incubation for 5 min at room temperature, 100 μL of 10 mM

ρ-nitrophenyl-α-D-glucoside solution was then added and incubated at 37 °C for another 20 min. After adding 250 µL of 100 mM sodium carbonate, the OD was measured at 405 nm using a visible-spectroscopy [38]. Phosphate buffer was used as a blank instead of the sample solution, while a positive control (Curcumin drug) was also involved. The α-glucosidase inhibition (%) was assayed using the following equation:

$$\alpha - \text{glucosidase inhibition}(\%) = \left[1 - \frac{\text{Abs}_{\text{sample}} - \text{Abs}_{\text{blank}}}{\text{Abs}_{\text{control}}}\right] \times 100 \quad (5)$$

where, $\text{Abs}_{\text{sample}}$, $\text{Abs}_{\text{blank}}$ and $\text{Abs}_{\text{control}}$ are the absorbance of the tested sample, blank and control, respectively.

2.8 Cytotoxicity and Anticancer Activity Assessments

The cytotoxic effect of the prepared Schiff base sample (CTS-SB) and chitosan (CTS) was tested for their compatibility to both normal somatic skin (HSF) cells and cancer hepatoma (HepG-2) cells using the MTT method with a slight modification [39, 40]. Both HSF and HepG-2 (1×10^4) cell lines were cultured in two sterile 96-well micro-plates for overnight in CO_2 incubator at 37 °C and 90% humidity. Both HSF and HepG-2 cell lines were treated with the prepared CTS-SB and CTS samples at different concentrations of 31.25, 62.5, 125, 250, 500 and 1000 µg/mL to the specific wells for 24 h and 72 h at the same conditions. After washing the cells three times with PBS, 200 µL of 0.5 mg/mL of MTT (dissolved in culture medium) was added to each well and incubated for 3 h at a proper circumstance. The MTT medium was aspirated and substituted with DMSO (200 µl/well) to dissolve crystal (purple formazan). The optical density (OD) was read at 590 nm using an ELISA microplate reader. Berberine was included at the same concentration as a standard drug. The cell viability of the prepared samples was presented as percentage of reference cells (untreated control cells), which was determined using the following equation:

$$\text{Cell viability}(\%) = \frac{\text{OD}_{\text{treated}}}{\text{OD}_{\text{reference}}} \times 10 \quad (7)$$

2.9 Cytocompatibility Test

Compatibility of the synthetized derivatives with the human blood was inspected according to the earlier reported procedure with a minor modification [15]. In brief, 0.1 g of tested sample was placed in saline phosphate buffer solution (PBS; 7 mL; pH 7.0) and left for incubation at 37 °C for 72 h. Next, the PBS was detached and 3 mL of citrate-dextrose solution (ACD) comprising 1 mL of anticoagulant and 9 mL of fresh blood was subsequently added to each sample and preserved at 37 ˚C for 3 h. Positive and negative controls were prepared by adding the same amount of ACD blood to 7 mL of water and PBS, respectively. Each tube was gently inverted twice each 30 min to maintain contact of the blood with the material. After incubation, each fluid was centrifuged at 2000 rpm for 15 min. The hemoglobin released by hemolysis was assayed via the estimation of the optical densities (OD) of the supernatants at 540 nm using a visible-spectroscopy.

$$\text{Hemolysis}\ (\%) = \frac{\text{OD}_s - \text{OD}_n}{\text{OD}_p - \text{OD}_n} \times 100 \quad (8)$$

where, ODs signifies the optical density of supernatant in the existence of examined sample, ODn and ODp are the optical densities of the negative and positive controls, respectively.

For blood test, informed consent was attained from a volunteer before the use of his blood for compatibility test. This research was approved by the ethical local committee at the General Authority of the SRTA-City, Egypt. In addition, all methods were performed in accordance with the relevant guidelines and regulations.

2.10 Statistical Analysis

All experiments were performed in triplicate, and the results were expressed as the mean standard deviation (± SD). Data were analyzed using two-way analysis of variance (ANOVA) and the significant data were determined at P-value < 0.05.

3 Results and Discussion

3.1 Chemistry

^{1}H NMR spectrum of CTS-SB derivative adopted in Fig. 2a displays the characteristic chemical shifts of protons of sulphanilimed moiety at δ 7.41, 6.55 and 5.81 ppm, which corresponding to two duplet of aromatic and NH_2 group of sulfanilamide in ratio (1:1:1). In addition, the strong peaks at δ 1.66 correspond to the aliphatic proton of dimedone moiety. Moreover, a huge peak appear at range δ 5.0–3.0 ppm correspond to the chitosan protons [41, 42].

FT-IR spectra were performed to get more details regarding the chemical structure of the synthesized CTS-SB derivative. Figure 2b reveals the spectra of neat chitosan and its Schiff base derivative. The CTS spectrum illustrated that typical bands of polysaccharides were detected [43, 44]. The observed bands between 3300 and 3500 cm^{-1} could be ascribed to OH and NH_2 groups, while bands at 2920 cm^{-1} are associated to the stretching vibration of CH_2 groups. Furthermore, the absorption bands at 1654 and 1540 cm^{-1} are

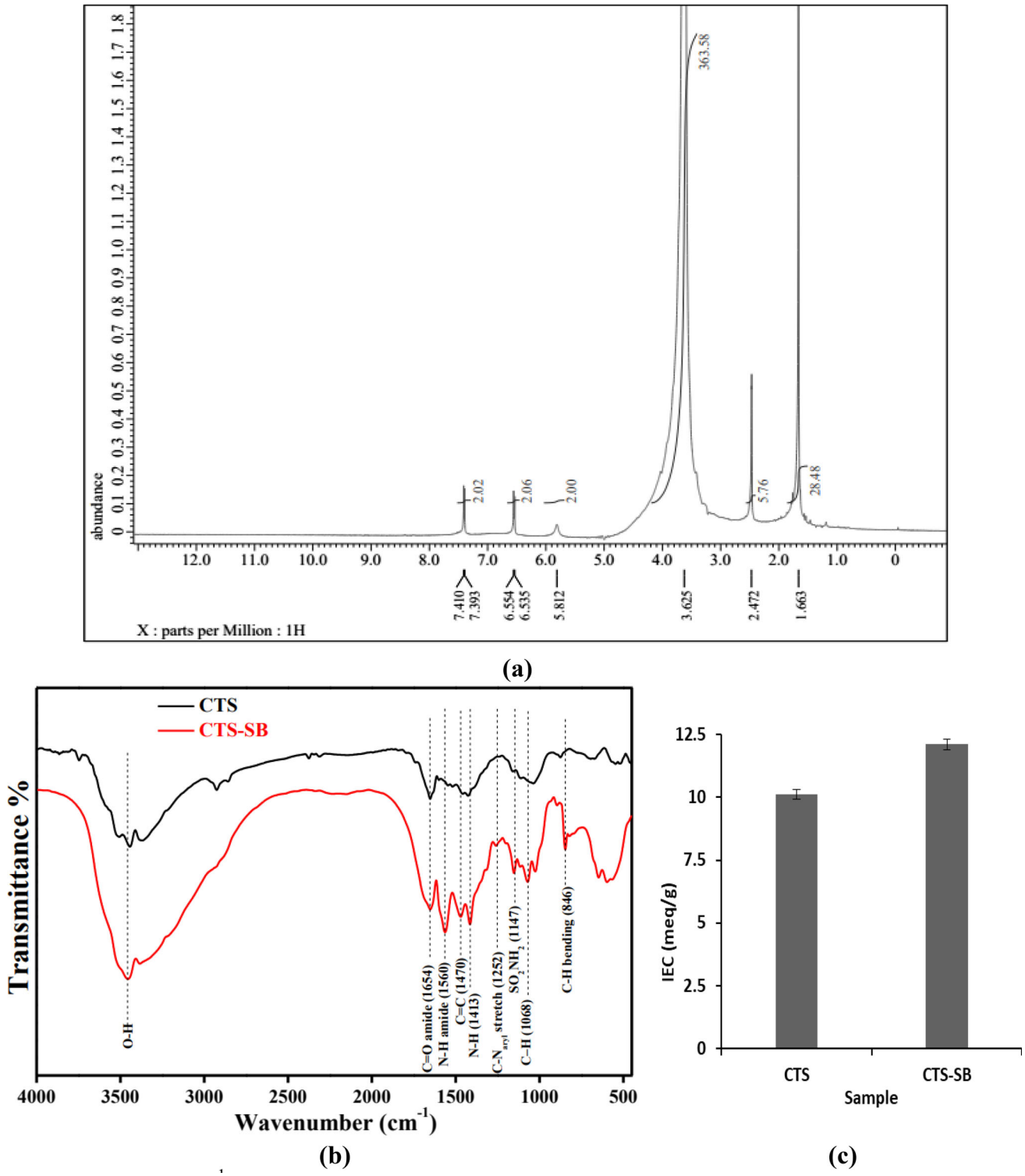

Fig. 2 **a** H^1 NMR spectrum of CTS-SB, **b** FT-IR spectra and **c** IEC values of native CTS and CTS-SB derivative

associated with the stretching vibration of C=O and N–H of amide-I and amide-II, respectively. The weak absorption peaks at 2850 cm^{-1} are assigned to C–H stretching vibrations. However, upon the formation of CTS-SB, the peak at 1654 cm^{-1} became more intense which could be attributed to the newly formed imine groups (C=N) and the peak at 3445 cm^{-1} was shifted to 3457 cm^{-1} [20, 22]. In addition, the observed peak at 1560 cm^{-1} became more intense due to the formed N–H amide groups. Besides, an obvious peaks assigned to aromatic moieties were appeared at 1470, 1068 and 840 cm^{-1}, which attributed to C=C, in-plane C–H bending and aromatic C–H bending [25]. Moreover, the IR spectrum of CTS-SB derivative showed characteristic bands at 1147 and 1309 cm^{-1}, which assigned to SO_2NH_2, while the observed strong peak at 1252 cm^{-1} could be attributed to the aryl C–N stretching. Accordingly, the gained results confirms the successful synthesis of CTS-SB derivative.

Besides, ion exchange capacity (IEC) measurement can be also taken as an indicator for Schiff base formation via the reactive NH_2 groups of CTS biopolymer. Figure 2c illustrates the results of IEC measurements for CTS and its Schiff base derivative. The results referred that CTS-SB derivative displayed higher IEC value of 12.1 meq/g compared to 10.1 meq/g for un-modified CTS. Increasing IEC value of CTS-SB derivative could be ascribed to increasing number of the primary and secondary amine groups on the backbone of chitosan after the Schiff base formation. The reversible nature of imine bonds renders its potential bioactivities for diverse biomedical applications.

3.2 Thermal Properties

The thermal stabilities of the synthetized CTS-SB derivative were established by TGA instrument with elevating temperature from 25 to 800 °C. The results demonstrated that thermograms of CTS and CTS-SB took place in three subsequent degradation stages. As presented in Table 1, the first weight loss was accrued with rising the temperature up to 120 °C, which caused by evaporation of the moisture content from the studied samples with maximum weight loss values reached 6.28 and 7.77% for CTS and CTS-SB derivative, respectively [45]. The second depression stage was accomplished with increasing temperature from 200 to 350 °C, which ascribed to the deformation of the glycoside bonds and breakdown of the pyranose ring [46]. The results signified that CTS-SB derivative displayed lower weight loss value of 21.31% compared to neat CTS which recorded 24.48%. The thermal stability was clearly observed from estimation of the temperature required for sample to loss its half weight ($T_{50\%}$ °C), which was higher in case of CTS-SB (481.1 °C) sample than pristine CTS (466.2 °C). Lastly, the third depression stage was perceived with increasing temperature up to 800 °C, and caused by dissociation of adducts and it. The detected degradation stages were matched with the previously reported thermal decomposition profile of chitosan polysaccharide and its derivatives [8, 12]. These results supposed the fair thermal stability in the vicinity of the temperature of human body, which boosts the potential application of CTS-SB derivative for biomedical fields such as drug delivery and wound dressing.

3.3 Surface Morphologies

The changes of the surface morphology of chitosan and its Schiff base were examined by SEM analysis at constant magnifications (× 1000 and × 5000) as depicted in Fig. 3. Noticeably, a sheet-like surface was observed in case of pure CTS biopolymer with a slight roughness (Fig. 3A, B). On the other hand, the surface roughness was increased in case of CTS-SB derivative, which exposed a rod-like structure with irregular particles and wrinkles (Fig. 3C–F). Introducing new functionalities on CTS backbone along with the polarity difference between CTS and CTS-SB could alter the internal chain order and consequently, bothered its crystal structure [47]. Indeed, surface roughness facilitates bacterial adhesion, which consequently promotes the inhibition of the bacterial growth [48].

3.4 Evaluation of Antibacterial Activity

Antibacterial activities of CTS and CTS-SB derivative against *E. coli* as Gram-negative bacteria and *S. aureus* as Gram-positive bacteria as shown in Fig. 4a. The results implied that the synthetized CTS-SB derivative demonstrated remarkable activities against the two examined bacteria as compared to pure CTS sample. In addition, the inhibition rate for Gram-positive bacteria was obviously higher than Gram-negative bacteria. Therefore, maximum inhibition (%) values of 84 and 61% were perceived against *S. aureus* and accomplished by CTS and CTS-SB derivative, respectively, while 71 and 49% were recorded by pure CTS. Definitely, the mechanism of antibacterial activity of chitosan is not yet completely understood, and thus, three inhibition mechanisms have been suggested [49]. The first mechanism includes the electrostatic attraction between the positive charge amine groups (NH_3^+) of chitosan and the negative charges on the cell wall of bacteria, which consequently which incites leakage of intracellular ingredients. The second mechanism concerned with the chelating capability of chitosan toward metal ions such as Ca^{2+}, Mg^{2+}, and Zn^{2+} [50]. These metal ions are necessary for bacterial growth in addition to their role in the metabolic pathways such as spore formation in Gram-positive bacteria. The third mechanism is associated with the penetration of the low chitosan molecular weight into the nuclei of microorganisms, which consequently can bind with DNA, suppress the mRNA

Table 1 TGA data for neat CTS and its Schiff base derivative (CTS-SB)

Sample	Weight loss (%)			$T_{50\%}$ (°C)
	1st depression 25–120 °C	2nd depression 200–350 °C	3rd depression 350–800 °C	
CTS	6.28	24.48	36.55	466.2
CTS-SB	7.77	21.31	29.2	481.1

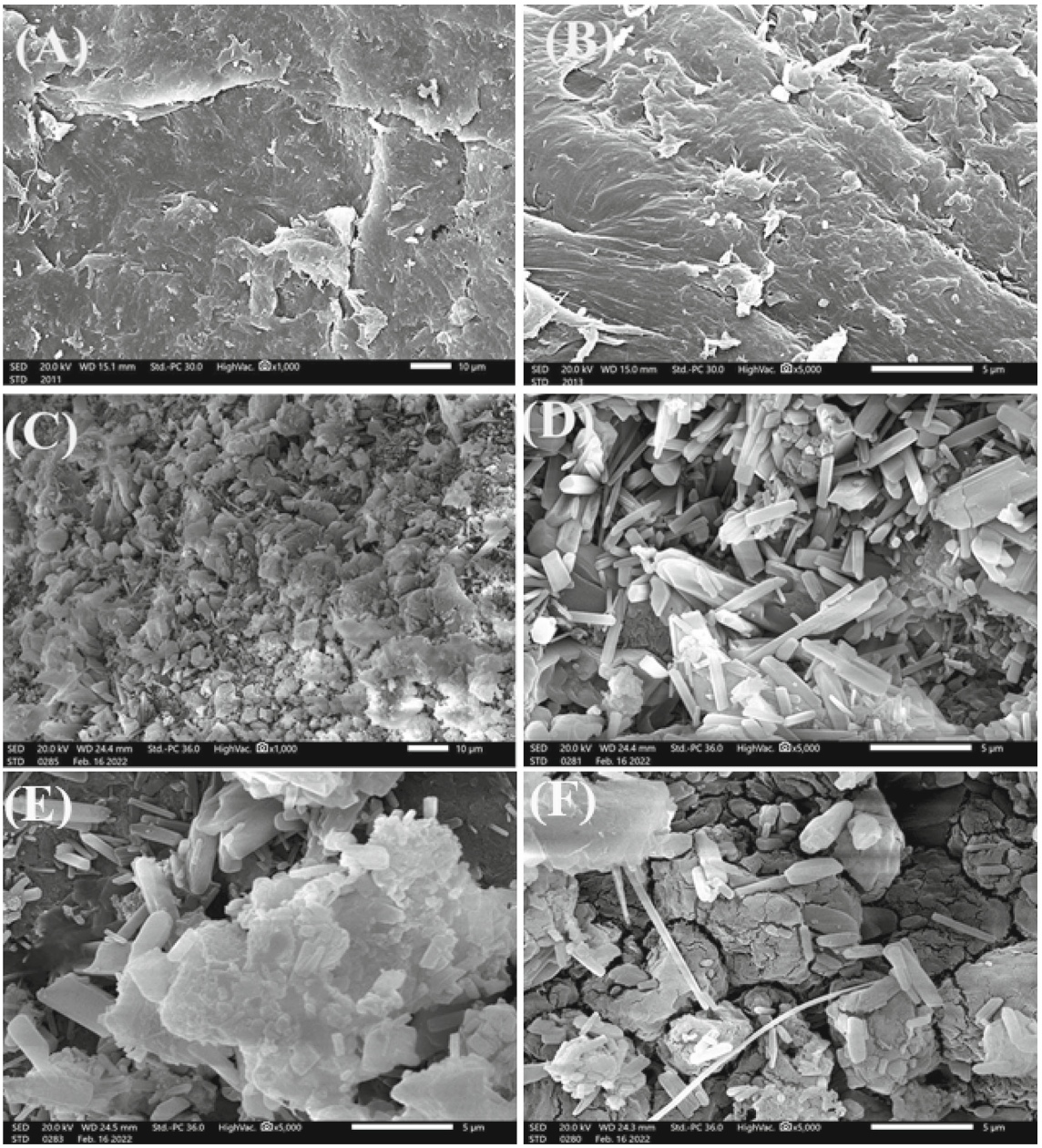

Fig. 3 SEM images of **A, B** neat CTS and **C, D, E, F** CTS-SB derivative

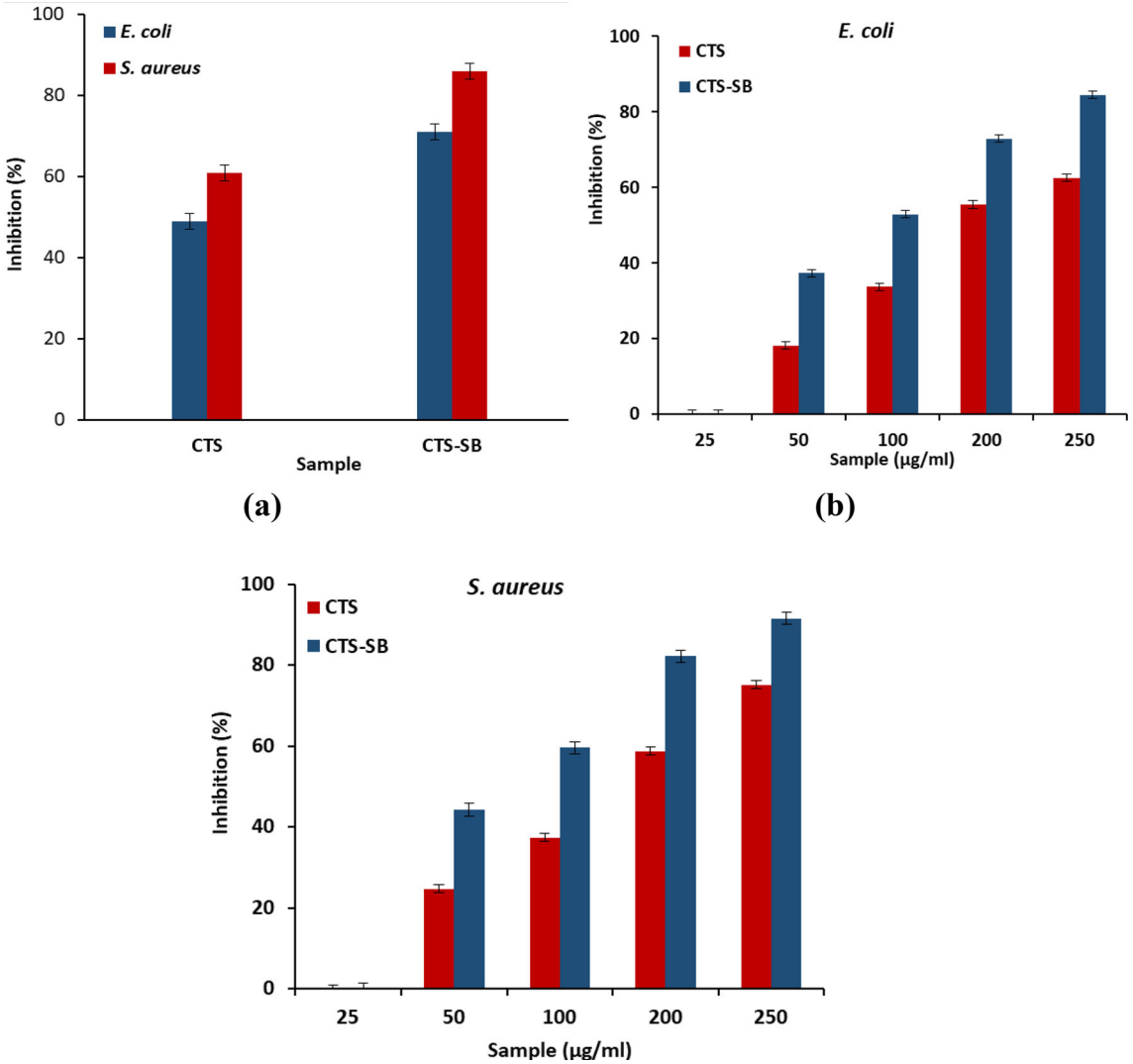

Fig. 4 **(a)** Antibacterial activities of CTS and CTS-SB derivative. MIC results of different concentrations of CTS and CTS-SB derivative against **(b)** *E. coli* and **(c)** *S. aureus.* All measurements were accomplished in triplicate ($n = 3$), and data obtained were expressed as mean standard deviation (± SD)

expression and prevent the protein synthesis, resulting in death of the bacterial cells occur. Increasing the antibacterial activity of chitosan Schiff base could be explained by generation of new Schiff base bond as well as introducing of some hydrophobic characteristics a long CTS backbone, which improves the interaction with peptidoglycan of the cell wall and lipoprotein in the outer membrane in addition to blocking the feeding channels responsible for exchanging of electrolytes/nutrients, resulting an increase in the inhibition rate of bacterial growth [51].

Similar observations have been reported by other researchers, for instance, the prepared chitosan Schiff bases (CSSBs) from the interaction of chitosan with acetophenone derivatives (4-aminoacetophenone enone and 4-bromoacetophenone), respectively. The synthetized CSSBs demonstrated remarkable antimicrobial activities compared with unmodified chitosan due to the generated electron-donating nature [52]. Similarly, a new chitosan Schiff base synthetized from an aldehyde revealed better antimicrobial properties owing to the electron-withdrawing substituents [23]. Further study proved that CSSB-1 and CSSB-2 resultant from the reaction of chitosan with 4-(2-chloroethyl) benzaldehyde (aldehyde-1) and 4-(bromoethyl) benzaldehyde (aldehyde-2), respectively had better activities against *S. aureus* and *P. aeruginosa* with doses of 0.006 and 0.012% [53]. These results were related to the present positively charged amine groups of CSSB-1 and CSSB-2, which have the capability for binding with the negatively charged surface of bacterial wall, leading to alteration of cell permeability and followed by cell death.

3.5 MIC Determination

On the other hand, minimum inhibitory concentration (MIC) of bioactive materials is considered one of the most vital parameters for using the antimicrobial agents to reduce their un-favorable properties as well as to examine the vulnerabilities of bacteria to the examined materials [54]. Herein, we have examined the lowest concentrations that could overpower the growth bacteria using different concentrations (25–250 μg/mL) for CTS-SB derivative in a comparison with the parent CTS biopolymer. As shown in Fig. 4b, c, typical behaviors of bacterial growth inhibition were accomplished. The results clarified that increasing concentrations of tested CTS and CTS-SB samples up to 250 μg/mL gradually boosted their inhibition activities. In addition, both of CTS and CTS-SB samples did not show any activity against *E. coli* and *S. aureus* bacteria at the lowest concentration (25 μg/mL). MIC was perceived at 50 μg/mL for CTS and CTS-SB derivative with maximum inhibition values reached 18 and 37%, respectively, against Gram negative *E. coli*, while approximately 24 and 44% were perceived against *S. aureus* bacteria. Therefore, maximal inhibition values of 84% (*E. coli*) and 91% (*S. aureus*) were obtained using 250 μg/mL of CTS-SB derivative. In fact, the higher activity of chitosan Schiff base against Gram-positive bacteria than Gram-negative bacteria could be attributed to the difference in the bacterial cell wall structures. These antibacterial manners are in reliable with the other previous studies [12, 22]. In addition, the existence of multi-barrier membranes in Gram-negative bacteria could slightly hinder the penetration of tested samples into the cells which involve the hydrophobic outer membrane, peptidoglycan layer and cell membrane. Furthermore, Gram-positive bacteria display thick peptidoglycan comprising teichoic acid molecules with negative charges, which can bind with the positively charged amine groups of CTS and CTS-SB derivative. Likewise, the structure of Gram-positive bacteria induces their ability to bind with CTS and its derivative, and consequently causes a destruction of bacterial cells. We could infer from these findings that the synthetized chitosan Schiff base (CTS-SB) derivative demonstrated outstanding antibacterial powerful, suggesting its potential use for biomedical applications [55].

3.6 Evaluation of Antidiabetic Activity

3.6.1 Glucose Uptake Evaluation

Figure 5 displays the results of glucose uptake by HepG-2 and Yeast cells in the presence of the examined CTS and its Schiff base derivative at different concentrations. The results signified that CTS-SB derivative has the aptitude to cause an obvious increase in glucose uptake by HepG-2 cells and yeast cells at all studied concentrations in a concentration-dependent manner as compared to the untreated control cells and/or native CTS. However, using berberine as a standard drug showed low increase levels in glucose uptake by both cells. Therefore, much higher increase in glucose uptake in yeast cells (Fig. 5a) was gained by CTS-SB derivative at 50 μg/mL with a maximal value of 52.53% compared to 19.2 and 41.45% for CTS and berberine drug, respectively. The prepared CTS-SB derivative also exhibited much higher increase in glucose uptake at 50 μg/mL by 39.6% in HepG-2 cells (Fig. 5b), while only 18.8 and 24.8% were recorded by pristine CTS and berberine, respectively. These observations clearly proposed that the synthetized CTS-SB derivative can effectively stimulates the glucose uptake by yeast cells more than berberine and pure CTS. Previous studies reported that chitosan derivatives potentially improved the general situation and diabetic symptoms of diabetic rats, decrease the blood glucose levels, and normalize the impaired insulin sensitivity [56]. Further, chitosan and its oligosaccharides act as antidiabetic agents for treatment of diabetes in manner of protecting pancreatic beta-cells. Additionally, it has been stated that chitosan derivatives improved glucose tolerance in STZ-induced diabetic mice with high-calorie diet [57]. Accordingly, CTS-SB derivative is suggested to acts as a regulator for the blood glucose level through improving the effective glucose uptake.

3.6.2 Inhibition of α-Amylase and α-Glucosidase

A-amylase and α-glucosidase inhibitions by CTS and CTS-SB derivative were deliberated in Table 2. The results indicated that CTS-SB derivative and acarbose/or curcumin exhibited potent α-amylase and α-glucosidase inhibitory activities than native CTS at all studied concentrations. Our results indicated that the α-amylase inhibitory activity increased gradually from 14.5 to 57.9% with raising the concentration from 15 to 249 mg/ml, while an increase from 55 to 49.8% was observed by native CTS sample [38]. Furthermore, the α-glucosidase inhibitory activity recorded maximum value of 53.44 and 63.92% at the highest used concentration (240 mg/mL) and obtained by CTS and CTS-SB, respectively.

Similar reports revealed that chitosan and its derivatives also demonstrated anti-diabetes activities, comprising anti-α-amylase and anti-α-glucosidase capability, making it a prospective candidate for anti-diabetic drug application [58, 59].

Therefore, chitosan and its derivatives have positive anti-diabetic benefits which are mediated through mechanisms including suppression of α-amylase and α-glucosidase activities, improving glucose metabolism, hindering intestinal glucose breakdown and decreasing β-cell dysfunction [60]. Also, water-soluble chitosan–glucose derivatives

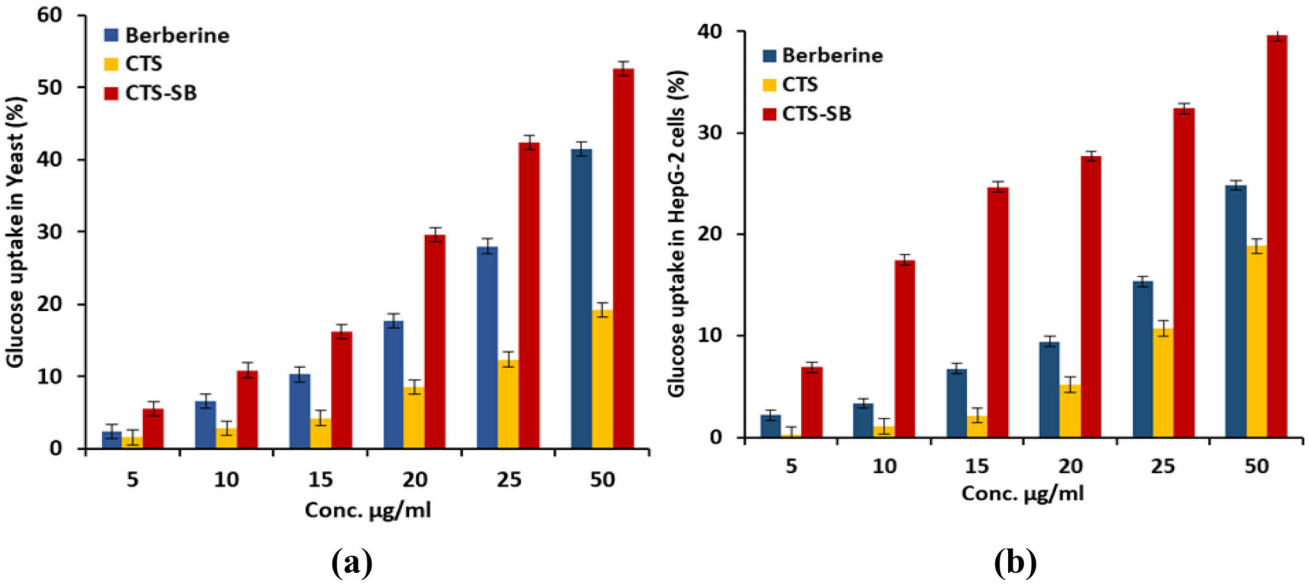

Fig. 5 Effect of pristine CTS and CTS-SB derivative on glucose utilization in **a** Yeast cells, **b** HepG-2 cells. Cells were treated for 48 and 3 h, respectively (berberine as a standard drug). Data are expressed as mean standard deviation (± SD)

Table 2 The inhibition effect of CTS and CTS-SB derivative on α-amylase and α-glucosidase activities (Acarbose and Curcumin as inhibitors for α-amylase and α-glucosidase, respectively)

Conc. (µg/mL)	α − amylase inhibition (%)			α − glucosidase inhibition (%)		
	Acarbose	CTS	CTS-SB	Curcumin	CTS	CTS-SB
15	6.41	3.544567	7.449824	27.86	8.33211	17.5982
30	12.11	6.55829	14.53344	43.51	17.88322	23.4663
60	35.34	16.07454	21.64816	58.79	25.34451	34.7608
120	70.23	25.5908	31.82025	77.96	33.11463	46.4816
180	84.77	37.70552	45.99233	87.52	41.10923	54.233
240	89.06	49.82025	57.93497	92.44	53.4489	63.97

Data are expressed as mean standard deviation (± SD)

(WSCGDs) have been reported to have anti -α-amylase and -α-glucosidase activities [58]. In accordance with these findings, the newly synthetized CTS-SB derivative had a reputable potential for inhibition of both α-amylase and α-glucosidase [27].

3.7 Anticancer Effect and Cytotoxicity Evaluation

In vitro cytotoxicity of the prepared CTS-SB sample was determined by the colorimetric MTT method against both normal and hepatoma cell lines at various concentrations in comparison with chitosan (CTS) and berberine samples. Our findings revealed that all tested samples showed a low level of cytotoxicity against normal HSF cells at all tested concentrations in a dose-dependent manner after treatment for 24 h and 72 h (Fig. 6A). However, the prepared CTS-SB sample at the highest concentrations (500 and 1000 µg/mL) showed about 50 and 35% of cells death after treatment for 24 and 72 h, respectively. Herein, the IC_{50} values of CTS-SB against HSF cells were determined to be 726.7 and 475.1 µg/mL after treatment for 24 and 72 h, respectively (Table 3). Our findings indicated that the safe doses (EC_{100}) of the prepared CTS and CTS-SB samples were determined to be ranged from 2.43 to 27.69 µg/mL after treatment for 24 and 72 h. However, IC_{50} values of CTS-SB against HepG-2 cells (Fig. 6B) were determined to be 109.6 and 76.74 µg/mL with SI values of 6.63 ± 0.10 and 6.19 after treatment for 24 and 72 h, respectively. These outcomes prove the significant safety for the prepared CTS-SB toward the normal human cells with high selectivity against hepatoma cancer cells [61, 62]. On the other hand, both chitosan (CTS) and berberine (standard drug) showed moderate antitumor activity against HepG-2 cells (Table 3). These results agreed with the previously reported studies. It has been reported that chitosan-quinolinone (CSQ), chitosan-pyranoquinolinone (CSP) Schiff bases and chitosan-quinolinone grafted on silver nanoparticles (CSQ/Ag) disclosed potent cytotoxic effect against three cancer cell HepG-2 cancerous cells [63].

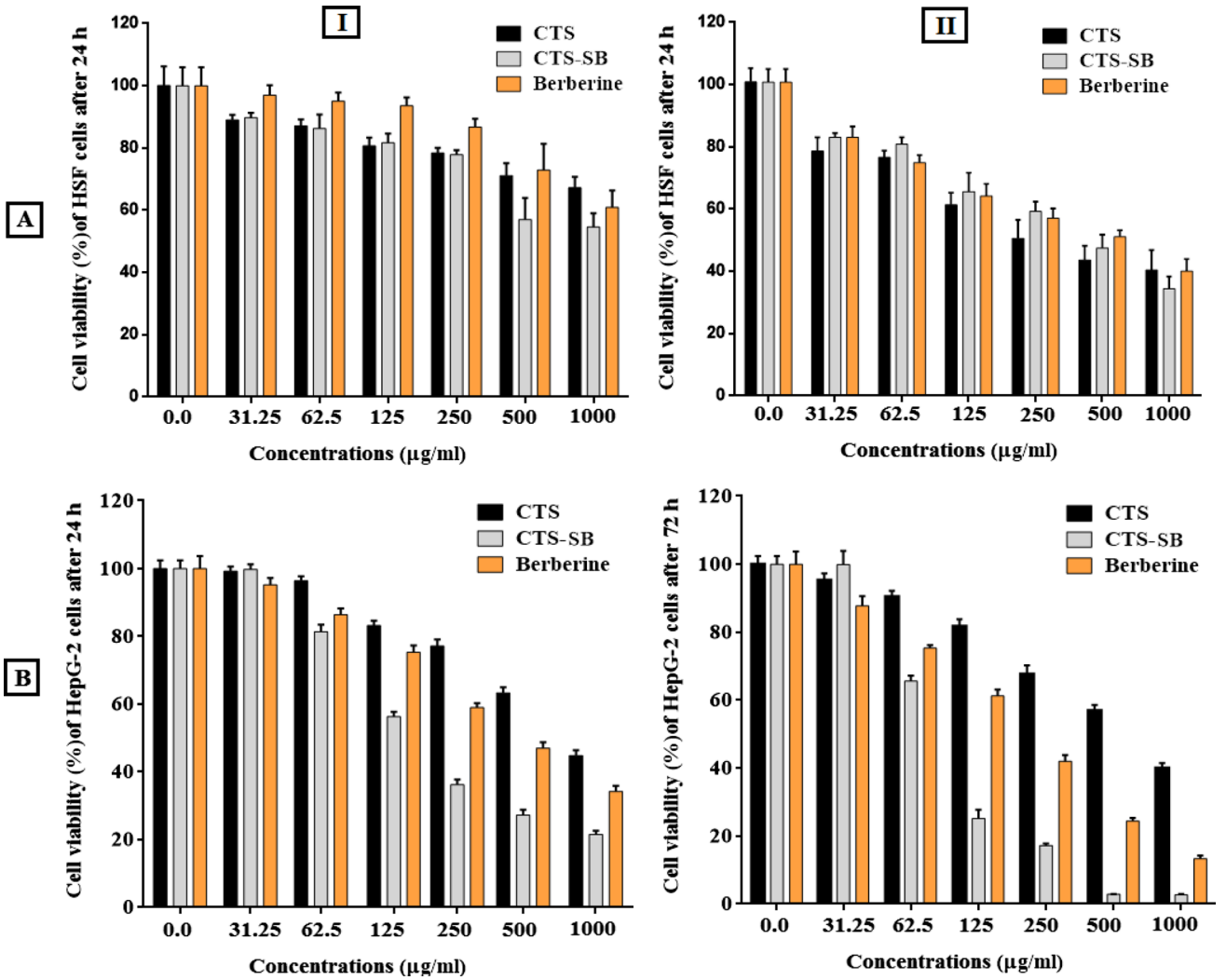

Fig. 6 Anticancer and cytotoxic effect of pristine CTS and CTS-SB derivative on viability of **A** normal HSF cells and **B** hepatoma HepG-2 cells as compared to CTS. Both HSF and HepG-2 cell lines were incubated with tested samples at various concentrations for 24 h (I) and 72 h (II). Berberine was included as positive standard drug. Data are expressed as mean standard deviation (± SD)

Table 3 The anticancer effect and cytotoxicity of pristine CTS and CTS-SB derivative against HepG-2 cells as compared to normal HSF cells expressed in EC_{100} (µg/ml), IC_{50} (µg/ml) and SI values

Sample		24 h		72 h	
		HSF	HepG-2	HSF	HepG-2
CTS	EC_{100}	27.69 ± 0.69	23.1 ± 0.45	15.41 ± 0.42	14.91 ± 0.28
	IC_{50}	875.21 ± 21.82	755.9 ± 4.51	487.0 ± 13.14	471.3 ± 8.82
	SI	–	1.16 ± 0.03	–	1.033 ± 0.02
CTS-SB	EC_{100}	22.99 ± 0.36	3.46 ± 0.41	15.03 ± 0.34	2.43 ± 0.08
	IC_{50}	726.7 ± 11.49	109.6 ± 4.13	475.1 ± 10.64	76.74 ± 2.46
	SI	–	6.63 ± 0.10	–	6.19 ± 0.14
Berberine	EC_{100}	17.52 ± 0.33	22.94 ± 0.21	11.69 ± 0.12	6.03 ± 0.04
	IC_{50}	553.9 ± 10.29	228.3 ± 2.06	369.4 ± 3.72	190.6 ± 1.29
	SI	–	2.43 ± 0.05	–	1.94 ± 0.02

All data are presented as the mean standard deviation (± SD)

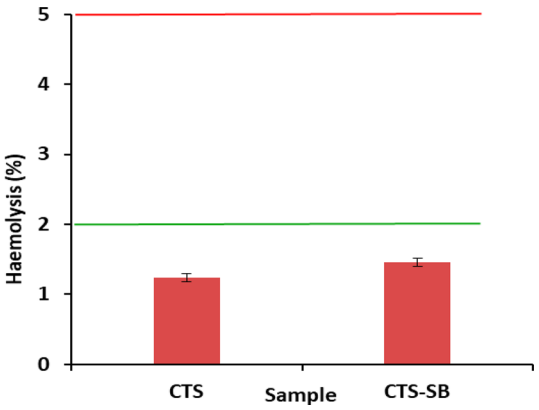

Fig. 7 Haemocompatibility of pristine CTS and CTS-SB derivative

Likewise, chitosan Schiff-base/ Cu complexes inhibited the growth of the liver cancer cell lines [64]. Moreover, the reported Schiff base derivative produced from sulphonylation of chitosan showed adequate anticancer activity via the inhibition of MCF-7 cells proliferation [65].

Factually, several mechanisms have been reported for clarifying the selectively permeation of chitosan and its derivatives through the cancer cell membranes. These mechanisms involve the cellular enzymatic, antioxidant defense mechanism, anti-angiogenic, immune-enhancing and apoptotic pathways. Collectively, CTS-SB derivative had the ability to exert more anticancer activity with high selectivity against HepG-2 cells more than pure CTS at all tested concentrations.

3.8 In Vitro Cytocompatibility

Biomaterials have been classified according to American Society for Testing and Materials (ASTM; F 756-00, 2000; US Pharmacopeia XXIII, 1994) into three classes namely; (i) non-hemolytic (hemolytic index < 2%), (ii) slightly hemolytic (hemolytic index of (2–5%) and (iii) hemolytic materials (hemolytic index over 5%) [45]. The synthetized CTS-SB derivative as well as neat CTS were tested their compatibilities as a function of the blood hemolysis (%). Figure 7 clarified that the examined CTS and CTS-SB derivative are safe and non-hemolylic materials, since they recorded minimal hemolysis values of 1.24 ± 0.83 and 1.46 ± 0.65% for CTS and CTS-SB samples, respectively. These findings confirm the outstanding compatibility of the developed derivatives which could be ascribed to the compatibility nature of native chitosan biopolymer [7]. In addition, coupling of chitosan with bioactive heterocyclic compounds induce some hydrophobic nature as a results of the existence of hydrophobic aromatic rings, and consequently, improves its compatibility. Similar results have been reported by other researches [66, 67].

4 Conclusion

A new bioactive Schiff base derivative was successfully synthetized through coupling of chitosan biopolymer with sulfonamide derivative, for boosting the antibacterial, anticancer and antioxidant activities of pristine chitosan. The CTS-SB derivative was characterized using various characterization tools, while IEC of CTS (10.1 meq/g) was augmented and reached 12.1 meq/g. In addition, CTS-SB demonstrated outstanding antibacterial activity against Gram-negative (*Escherichia coli*) and Gram-positive (*Staphylococcus aureus)* bacteria, while MIC value was perceived at 50 μg/mL. Furthermore, CTS-SB derivative proved its capability of inhibiting both α-amylase and α-glucosidase activity in diabetic patients together with inhibitory values reached 57.9 and 63.9%, respectively. A significant anticancer activity with high selectivity was detected against HepG-2 cells with safety margin. Besides, CTS-SB derivative demonstrated acceptable blood compatibility, suggesting its potential use for biomedical fields such as drug delivery and wound dressing.

Author Contributions AMO: Conceptualization, Methodology, Writing- Original draft preparation, Writing- Reviewing and Editing. ASE: Investigation, Writing- Reviewing and Editing. EMEF: Methodology, Writing- Reviewing and Editing. EMAE-M: Methodology, Formal analysis. MMFI: Writing- Reviewing and Editing. Mohamed S. Mohy-Eldin: Writing- Reviewing and Editing. MSA: Conceptualization, Methodology, Writing- Reviewing and Editing.

Funding Open access funding provided by The Science, Technology & Innovation Funding Authority (STDF) in cooperation with The Egyptian Knowledge Bank (EKB).

Data Availability The datasets generated during and/or analyzed during the current study are available from the corresponding author on reasonable request.

Declarations

Conflict of interest The authors declare that there is no conflict of interest associated with this manuscript.

References

1. George, A.; Sanjay, M.; Srisuk, R.; Parameswaranpillai, J.; Siengchin, S.: A comprehensive review on chemical properties and applications of biopolymers and their composites. Int. J. Biol. Macromol. **154**, 329–338 (2020)
2. Van de Velde, K.; Kiekens, P.: Biopolymers: overview of several properties and consequences on their applications. Polym. Test. **21**, 433–442 (2002)
3. Reddy, N.; Reddy, R.; Jiang, Q.: Crosslinking biopolymers for biomedical applications. Trends Biotechnol. **33**, 362–369 (2015)
4. Tamer, T.M.; Omer, A.M.; Hassan, M.A.; Hassan, M.E.; Sabet, M.M.; Mohy Eldin, M.S.: Development of thermo-sensitive poly N-isopropyl acrylamide grafted chitosan derivatives. J. Appl. Pharma. Sci. **5**, 1–6 (2015)
5. Rinaudo, M.: Chitin and chitosan: properties and applications. Prog. Polym. Sci. **31**, 603–632 (2006)
6. Hamedi, H.; Moradi, S.; Hudson, S.M.; Tonelli, A.E.; King, M.W.: Chitosan based bioadhesives for biomedical applications: a review. Carbohydr. Polym. **282**, 119100 (2022)
7. Dehshahri, A.; Khalvati, B.; Taheri, Z.; Safari, F.; Mohammadinejad, R.; Heydari, A.: Interleukin-12 plasmid DNA delivery by *N*-[(2-Hydroxy-3-trimethylammonium)propyl]chitosan-based nanoparticles. Polymers (Basel) **14**(11), 2176 (2022)
8. Mohy Eldin, M.S.; Omer, A.M.; Wassel, M.A.; Tamer, T.M.; AbdElmonem, M.S.; Ibrahim, S.A.: Novel smart pH sensitive chitosan grafted alginate hydrogel microcapsules for oral protein delivery: II. Evaluation of the swelling behavior. Int. J. Pharm. Pharm. Sci. **7**(10), 331–337 (2015)
9. Eltaweil, A.S.; Hashem, O.A.; Abdel-Hamid, H.; Abd El-Monaem, E.M.; Ayoup, M.S.: Synthesis of a new magnetic Sulfacetamide-Ethylacetoacetate hydrazone-chitosan Schiff-base for Cr(VI) removal. Int. J. Biol. Macromol. **222**, 1465–1475 (2022)
10. Hu, D.L.; Lian, Z.W.; Xian, H.Y.; Jiang, R.; Wang, N.; Weng, Y.Y.; Peng, X.W.; Wang, S.M.; Ouyang, X.K.: Adsorption of Pb(II) from aqueous solution by polyacrylic acid grafted magnetic chitosan nanocomposite. Int. J. Biol. Macromol. **154**, 1537–1547 (2020)
11. Yu, D., et al.: The microstructure, antibacterial and antitumor activities of chitosan oligosaccharides and derivatives. Mar. Drugs **20**, 69 (2022)
12. Hassan, M.A., et al.: Antioxidant and antibacterial polyelectrolyte wound dressing based on chitosan/hyaluronan/phosphatidylcholine dihydroquercetin. Int. J. Biol. Macromol. **166**, 18–31 (2021)
13. Hu, Z.; Zhang, D.-Y.; Lu, S.-T.; Li, P.-W.; Li, S.-D.: Chitosan-based composite materials for prospective hemostatic applications. Mar. Drugs **16**, 273 (2018)
14. Chang, P.-H.; Sekine, K.; Chao, H.-M.; Hsu, S.-H.; Chern, E.: Chitosan promotes cancer progression and stem cell properties in association with Wnt signaling in colon and hepatocellular carcinoma cells. Sci. Rep. **7**, 1–14 (2017)
15. Omer, A.M., et al.: Formulation and antibacterial activity evaluation of quaternized aminochitosan membrane for wound dressing applications. Polymers **13**, 2428 (2021)
16. Beceiro, A.; Tomás, M.; Bou, G.: Antimicrobial resistance and virulence: a successful or deleterious association in the bacterial world? Clin. Microbiol. Rev. **26**, 185–230 (2013)
17. Hassan, M.A.; Abol-Fotouh, D.; Omer, A.M.; Tamer, T.M.; Abbas, E.: Comprehensive insights into microbial keratinases and their implication in various biotechnological and industrial sectors: a review. Int. J. Biol. Macromol. **154**, 567–583 (2020)
18. Ji, J., et al.: Chemical modifications of chitosan and its applications. Polym.-Plast. Technol. Eng. **53**, 1494–1505 (2014)
19. Heydari, A.; Dušička, E.; Mičušík, M.; Sedlák, M.; Lacík, I.: Unexpected counterion exchange influencing fundamental characteristics of quaternary ammonium chitosan salt. Polymer **220**, 123562 (2021)
20. Omer, A.M.; Ammar, Y.; Mohamed, G.A.; Tamer, T.M.: Preparation of Isatin/chitosan schiff base as novel antibacterial biomaterials. Egypt. J. Chem. **62**, 123–131 (2019)
21. Mohamed, R.R.; Fekry, A.: Antimicrobial and anticorrosive activity of adsorbents based on chitosan Schiff's base. Int. J. Electrochem. Sci. **6**, 2488–2508 (2011)
22. Hassan, M.A.; Omer, A.M.; Abbas, E.; Baset, W.; Tamer, T.M.: Preparation, physicochemical characterization and antimicrobial activities of novel two phenolic chitosan Schiff base derivatives. Sci. Rep. **8**, 1–14 (2018)
23. Yin, X.; Chen, J.; Yuan, W.; Lin, Q.; Ji, L.; Liu, F.: Preparation and antibacterial activity of Schiff bases from O-carboxymethyl chitosan and para-substituted benzaldehydes. Polym. Bull. **68**(5), 1215–1226 (2012). https://doi.org/10.1007/s00289-011-0599-4
24. Montaser, A.S.; Wassel, A.R.; Al-Shaye'a, O.N.: Synthesis, characterization and antimicrobial activity of Schiff bases from chitosan and salicylaldehyde/TiO2 nanocomposite membrane. Int. J. Biol. Macromol. **124**, 802–809 (2019). https://doi.org/10.1016/j.ijbiomac.2018.11.229
25. Tamer, T.M., et al.: Synthesis, characterization and antimicrobial evaluation of two aromatic chitosan Schiff base derivatives. Process Biochem. **51**, 1721–1730 (2016)
26. Wang, R.M., et al.: Preparation of nano-chitosan Schiff-base copper complexes and their anticancer activity. Polym. Adv. Technol. **20**, 959–964 (2009)
27. Priyanka, D.N.; Prashanth, K.V.H.; Tharanathan, R.N.: A review on potential anti-diabetic mechanisms of chitosan and its derivatives. Carbohydr. Polym. Technol. Appl. **3**, 100188 (2022). https://doi.org/10.1016/j.carpta.2022.100188
28. Manimohan, M.; Pugalmani, S.; Sithique, M.A.: Biologically active water soluble novel biopolymer/hydrazide based O-carboxymethyl chitosan Schiff bases: synthesis and characterisation. J. Inorg. Organomet. Polym Mater. **30**, 3658–3676 (2020)
29. Pick, A.M.; Nystrom, K.K.: Pazopanib for the treatment of metastatic renal cell carcinoma. Clin. Ther. **34**, 511–520 (2012)
30. Ayoup, M.S.; Soliman, S.M.; Haukka, M.; Harras, M.F.; Menofy, N.G.; Ismail, M.M.: Prodrugs of sulfacetamide: synthesis, X-ray structure, Hirshfeld analysis, antibacterial assessment, and docking studies. J. Mol. Struct. **1251**, 132017 (2022)
31. Reynolds, R.M., et al.: Glibenclamide and metfoRmin versus stAndard care in gEstational diabeteS (GRACES): a feasibility open label randomised trial. BMC Pregnancy Childbirth **17**, 1–9 (2017)
32. Bishoyi, A.K.; Mahapatra, M.; Sahoo, C.R.; Paidesetty, S.K.; Padhy, R.N.: Design, molecular docking and antimicrobial assessment of newly synthesized p-cuminal-sulfonamide Schiff base derivatives. J. Mol. Struct. **1250**, 131824 (2022)
33. Awad, L.F.; Ayoup, M.S.: Fluorinated phenylalanines: synthesis and pharmaceutical applications. Beilstein J. Org. Chem. **16**, 1022–1050 (2020). https://doi.org/10.3762/bjoc.16.91
34. Ayoup, M.S.; Rabee, A.R.; Abdel-Hamid, H.; Harras, M.F.; El Menofy, N.G.; Ismail, M.M.F.: Exploration of nitroaromatic antibiotics via sanger's reagent: synthesis, in silico, and antimicrobial evaluation. ACS Omega **7**(6), 5254–5263 (2022). https://doi.org/10.1021/acsomega.1c06383
35. Rufián-Henares, J.A.; Morales, F.J.: Microtiter plate-based assay for screening antimicrobial activity of melanoidins against *E. coli* and *S. aureus*. Food Chem. **111**, 1069–1074 (2008)
36. Van de Venter, M., et al.: Antidiabetic screening and scoring of 11 plants traditionally used in South Africa. J. Ethnopharmacol. **119**, 81–86 (2008)
37. Hosny, M., et al.: Biogenic synthesis, characterization, antimicrobial, antioxidant, antidiabetic, and catalytic applications of

platinum nanoparticles synthesized from Polygonum salicifolium leaves. J. Environ. Chem. Eng. **10**, 106806 (2022)
38. Sancheti, S.; Sancheti, S.; Seo, S.-Y.: Evaluation of antiglycosidase and anticholinesterase activities of Boehmeria nivea. Pak. J. Pharm. Sci. **23**(2), 236–240 (2010)
39. Hosny, M.; Fawzy, M.; El-Badry, Y.A.; Hussein, E.E.; Eltaweil, A.S.: Plant-assisted synthesis of gold nanoparticles for photocatalytic, anticancer, and antioxidant applications. J. Saudi Chem. Soc. **26**(2), 101419 (2022)
40. El-Fakharany, E.M.; Saad, M.H.; Salem, M.S.; Sidkey, N.M.: Biochemical characterization and application of a novel lectin from the cyanobacterium Lyngabya confervoides MK012409 as an antiviral and anticancer agent. Int. J. Biol. Macromol. **161**, 417–430 (2020)
41. Hirai, A.; Odani, H.; Nakajima, A.: Determination of degree of deacetylation of chitosan by 1H NMR spectroscopy. Polym. Bull. **26**, 87–94 (1991)
42. Kasaai, M.R.: Determination of the degree of N-acetylation for chitin and chitosan by various NMR spectroscopy techniques: a review. Carbohyd. Polym. **79**, 801–810 (2010)
43. Pawlak, A.; Mucha, M.: Thermogravimetric and FTIR studies of chitosan blends. Thermochim. Acta **396**, 153–166 (2003)
44. Mohy Eldin, M.S.; Hashem, A.E.; Tamer, T.M.; Omer, A.M.; Yossuf, M.E.; Sabet, M.M.: Development of cross linked chitosan/alginate polyelectrolyte proton exchanger membranes for fuel cell applications. Int. J. Electrochem. Sci. **12**, 3840–3858 (2017)
45. Omer, A.M.; Ziora, Z.M.; Tamer, T.M.; Khalifa, R.E.; Hassan, M.A.; Mohy-Eldin, M.S.; Blaskovich, M.A.T.: Formulation of quaternized aminated chitosan nanoparticles for efficient encapsulation and slow release of curcumin. Molecules **26**, 449 (2021)
46. Ferreira, P.; Coelho, J.; Dos Santos, K.; Ferreira, E.; Gil, M.: Thermal characterization of chitosan-grafted membranes to be used as wound dressings. J. Carbohydr. Chem. **25**, 233–251 (2006)
47. Omer, A.M.; Ahmed, M.S.; El-Subruiti, G.M.; Khalifa, R.E.; Eltaweil, A.S.: pH-sensitive alginate/carboxymethyl chitosan/aminated chitosan microcapsules for efficient encapsulation and delivery of diclofenac sodium. Pharmaceutics **13**, 338 (2021)
48. Yoda, I.; Koseki, H.; Tomita, M., et al.: Effect of surface roughness of biomaterials on Staphylococcus epidermidis adhesion. BMC Microbiol. **14**, 234 (2014). https://doi.org/10.1186/s12866-014-0234-2
49. Li, J.; Zhuang, S.: Antibacterial activity of chitosan and its derivatives and their interaction mechanism with bacteria: current state and perspectives. Eur. Polymer J. **138**, 109984 (2020)
50. Malekshah, R.E.; Shakeri, F.; Aallaei, M.; Hemati, M.; Khaleghian, A.: Biological evaluation, proposed molecular mechanism through docking and molecular dynamic simulation of derivatives of chitosan. Int. J. Biol. Macromol. **166**, 948–966 (2021)
51. Helander, I.; Nurmiaho-Lassila, E.-L.; Ahvenainen, R.; Rhoades, J.; Roller, S.: Chitosan disrupts the barrier properties of the outer membrane of Gram-negative bacteria. Int. J. Food Microbiol. **71**, 235–244 (2001)
52. Raouf, O.H.; Selim, S.; Mohamed, H.; Abdel-Gawad, O.F.; Elzanaty, A.M.; Ahmed, S.A.-K.: Synthesis, characterization and biological activity of Schiff bases based on chitosan and acetophenone derivatives. Adv. J. Chem. A **3**, 274–282 (2020)
53. Fontana, R.; Marconi, P.C.R.; Caputo, A.; Gavalyan, V.B.: Novel chitosan-based Schiff base compounds: chemical characterization and antimicrobial activity. Molecules **27**, 2740 (2022). https://doi.org/10.3390/molecules27092740
54. Peng, Y.; Han, B.; Liu, W.; Xu, X.: Preparation and antimicrobial activity of hydroxypropyl chitosan. Carbohyd. Res. **340**, 1846–1851 (2005)
55. Martins, A.F., et al.: Characterization of N-trimethyl chitosan/alginate complexes and curcumin release. Int. J. Biol. Macromol. **57**, 174–184 (2013)
56. Karadeniz, F.; Kim, S.-K.: Chapter three - antidiabetic activities of chitosan and its derivatives: a mini review. Adv. Food Nutr Res **73**, 33–44 (2014). https://doi.org/10.1016/B978-0-12-800268-1.00003-2
57. Ju, C.; Yue, W.; Yang, Z.; Zhang, Q.; Yang, X.; Liu, Z.: Antidiabetic effect and mechanism of chitooligosaccharides. Biol. Pharm. Bull. **33**(9), 11516–15141 (2010). https://doi.org/10.1248/bpb.33.1511
58. Tran, T.N.; Doan, C.T.; Nguyen, V.B.; Nguyen, A.D.; Wang, S.L.: Anti-oxidant and anti-diabetes potential of water-soluble chitosan-glucose derivatives produced by maillard reaction. Polymers (Basel) **11**(10), 1714 (2019). https://doi.org/10.3390/polym11101714
59. Liu, J.; Lu, J.F.; Kan, J.; Jin, C.H.: Synthesis of chitosan-gallic acid conjugate: structure characterization and in vitro anti-diabetic potential. Int. J. Biol. Macromol. **62**, 321–329 (2013). https://doi.org/10.1016/j.ijbiomac.2013.09.032
60. Yu, S.Y.; Kwon, Y.I.; Lee, C.; Apostolidis, E.; Kim, Y.C.: Antidiabetic effect of chitosan oligosaccharide (GO2KA1) is mediated via inhibition of intestinal alpha-glucosidase and glucose transporters and PPARγ expression. BioFactors (Oxford, England) **43**(1), 90–99 (2017)
61. Mostafa, M.A.; Ismail, M.M.; Morsy, J.M.; Hassanin, H.M.; Abdelrazek, M.M.: Synthesis, characterization, anticancer, and antioxidant activities of chitosan Schiff bases bearing quinolinone or pyranoquinolinone and their silver nanoparticles derivatives. Polym. Bull. (2022). https://doi.org/10.1007/s00289-022-04238-7
62. Packialakshmi, P.; Gobinath, P.; Ali, D.; Alarifi, S.; Gurusamy, R.; Idhayadhulla, A.; Surendrakumar, R.: New chitosan polymer scaffold Schiff bases as potential cytotoxic activity: synthesis, molecular docking, and physiochemical characterization. Front. Chem. **9**, 796599 (2022). https://doi.org/10.3389/fchem.2021.796599
63. Adhikari, H.S.; Yadav, P.N.: Anticancer activity of chitosan, chitosan derivatives, and their mechanism of action. Int. J. Biomater. **30**, 2952085 (2018). https://doi.org/10.1155/2018/2952085
64. Wang, R.M.; He, N.P.; Song, P.F.; He, Y.F.; Ding, L.; Lei, Z.Q.: Preparation of nano-chitosan Schiff-base copper complexes and their anticancer activity. Polym. Adv. Technol. **20**(12), 959–964 (2008). https://doi.org/10.1007/s00289-011-0599-4
65. Jiang, M.; Ouyang, H.; Ruan, P., et al.: Chitosan derivatives inhibit cell proliferation and induce apoptosis in breast cancer cells. Anticancer Res. **31**(4), 1321–1328 (2011)
66. Tihan, G.; Zgarian, R.G.; Berteanu, E.; Ionita, D.; Totea, G.; Iordachel, C.; Tatia, R.; Prodana, M.; Demetrescu, I.: Alkaline phosphatase immobilization on new chitosan membranes with Mg2+ for biomedical applications. Mar. Drugs **16**, 287 (2018)
67. Guo, X.; Sun, T.; Zhong, R.; Ma, L.; You, C.; Tian, M.; Li, H.; Wang, C.: Effects of chitosan oligosaccharides on human blood components. Front. Pharmacol. **9**, 1412 (2018)